Desalination and Water Treatment
www.deswater.com
doi: 10.1080/19443994.2015.1081625

57 (2016) 16559–16570
July

Taylor & Francis
Taylor & Francis Group

Biosorption of Cd(II) by *Pleurotus mutilus* biomass in fixed-bed column: experimental and breakthrough curves analysis

Mohamed Khitous[a,b,*], Samir Moussous[c], Ammar Selatnia[b], Mohamed Kherat[a,b]

[a]*Centre de Développement des Energies Renouvelables CDER, BP 62 Route de l'observatoire, Bouzaréah, Algiers 16340, Algeria, Tel. +213 219 01503; emails: usthbkhitous@yahoo.fr (M. Khitous), m.kherat@cder.dz (M. Kherat)*
[b]*Département de Génie Chimique, Ecole Nationale Polytechnique, 10 Avenue Hassen Badi, BP 182, El Harrach, Algiers, Algeria, Tel. +213 215 22973; email: ammarselatnia@yahoo.fr (A. Selatnia)*
[c]*Laboratoire d'Electrochimie et de Corrosion, Ecole Militaire Polytechnique, BP 17 Bordj-El-Bahri, Algiers 16111, Algeria, Tel. +213 215 22973; email: mou162003@yahoo.fr*

Received 16 October 2014; Accepted 2 August 2015

ABSTRACT

The removal of Cd(II) from aqueous solutions by a *Pleurotus mutilus* macrofungal biomass was investigated in a fixed-bed column. The experiments were conducted to study the effects of important design parameters such as bed depth (10–15 cm), flow rate (5–20 mL/min), and inlet concentration (30–50 mg/L). The optimum conditions were achieved at 15 cm, 10 mL/min, and 50 mg/L, respectively. The BDST, Thomas, and Adams–Bohart models were also applied to the experimental data to predict the breakthrough curves at various operating parameters. The BDST model was in good agreement with the experimental data. The breakthrough curves were well fitted with the Thomas model ($R^2 > 0.97$), while the Adams–Bohart model was applicable for the initial part of biosorption. The column was regenerated by eluting Cd(II) using 0.05 M HNO_3 and the biosorbent was reused for three biosorption regeneration cycles. The results show a good regeneration efficiency and a high removal for Cd(II) with a slight decrease in biosorption capacity with cycles. *P. mutilus* macrofungal biomass was proved to be a potential biosorbent for the removal of Cd(II) in the fixed-bed column.

Keywords: Pleurotus mutilus; Cd(II); Biosorption; Modeling; Fixed-bed column

1. Introduction

Cadmium is one of the most toxic pollutants in wastewater that is introduced into water from metal mining, plating, batteries, pesticides, and pigments [1,2]. It is considered to be particularly toxic and responsible for the serious decrease in biological activity [3,4]. Cd(II) is accumulated in the kidneys and liver, and ingestion results in several diseases such as epigastric pain, nausea, vomiting, severe diarrhea, and hemorrhage [5]. The World Health Organization has set a maximum guideline concentration of 0.003 mg/L for Cd(II) in drinking water [6].

The most widely used physicochemical methods for cadmium removal include ion exchange [7], chemical precipitation [8], coagulation–flocculation [9], membrane filtration [10,11], and electrochemical treatment [12]. However, most of these methods suffer from some drawbacks, such as high operating cost,

*Corresponding author.

incomplete precipitation, and sludge generation, and are not suitable for small-scale industries [13]. In comparison with the conventional methods, biosorption is usually preferred due to its high efficiency, easy handling, availability of various biosorbents, selective adsorption of metal ions, short operation time, and the possibility of material regeneration [14]. Although the use of activated carbon for cadmium removal has been found to be successful [15,16], its application has been limited because of its high cost and regeneration difficulties [17,18]. Consequently, it is important to find low-cost and non-conventional alternative materials instead of traditional biosorbents. Recently, some industrial byproducts, agricultural residues, and forestry resources have received considerable attention for application as biosorbents for Cd(II) removal [19–26].

The edible fungus *Clitopilus scyphoides* (formerly *Pleurotus mutilus*) is used by the SAIDAL industrial complex in Médéa (Algeria) for the production of pleuromutilin antibiotic. Large amounts of fungal residue (35 tons/years) are produced during the fermentation process and discharged to landfill with no valorization. Previously, many studies have reported the use of fungal residues (*C. scyphoides*) as biosorbents. Chergui et al. [27] presented the main physicochemical features of the dead fungal biomass of the basidiomycete *P. mutilus*, and tested it as a biosorbent to remove the hexacyanoferrate (III) complex anions. Later on, Yeddou-Mezenner [28] investigated the ability of the fungal residue to adsorb the cationic dye Basic Blue 41. In our previous study, we investigated the biosorption of cadmium by an industrial residue of macrofungal biomass (*C. scyphoides*) in batch mode [29]. We studied the effect of various operating conditions such as the solution pH, initial concentration of the test solution, and biosorbent dosage. The effect of other metal concentrations on the biosorption capacity was also investigated. However, studies on this biosorbent so far have been restricted to batch systems only. Batch mode is not convenient for application in an industrial scale, in which large volumes of wastewater are continuously generated. Therefore, further investigations are warranted to establish its potential under a continuous mode using fixed-bed column.

In process applications, a fixed-bed column is simple to operate and economically valuable for wastewater treatment [30–32]. Data obtained from experiments using a laboratory-scale fixed-bed column with a relatively large volume can be used to design a larger pilot and industrial scale plant with a high degree of accuracy [33].

Therefore, this investigation was aimed at studying the continuous biosorption of cadmium by a *P. mutilus* biomass in a fixed-bed column, and to determine the optimal operating conditions (flow rate, inlet feed concentration, and bed depth). Moreover, the experimental breakthrough curves were fitted to the adsorption models, such as the Thomas, Adams–Bohart, and bed depth service time (BDST) models, to determine useful characteristic parameters for process design.

2. Materials and methods

2.1. Biosorbent preparation and characterization

2.1.1. Biosorbent preparation

The industrial fungal waste, obtained after pleuromutilin extraction from *P. mutilus* biomass, was obtained from the SAIDAL antibiotic production complex in Médéa (Algeria). This waste, collected as wet flocs with yellowish color and a characteristic odor, was thoroughly washed with distilled water and dried for 24 h at 50°C in an oven. The dried residue was grounded manually in a mortar, sieved to yield particles of 315–400 μm size, and stored at room temperature before characterization and biosorption experiments.

2.1.2. Biosorbent characterization

2.1.2.1. Apparent density and specific surface area. The apparent density of the biosorbent was determined using a pycnometer and the specific surface area was calculated using the following equation:

$$S_p = \frac{6}{\rho_{app} d_p} \quad (1)$$

where d_p (μm) is the mean diameter of biosorbent particles (assumed to be spherical), S_p (m^2/g) is the specific surface area of biosorbent, and ρ_{app} (g/m^3) is the apparent density of the biosorbent. The physicochemical characteristics of the biosorbent are listed in Table 1.

2.1.2.2. Scanning electron microscopy, Fourier transform infrared, and X-ray fluorescence analyses. The surface morphology of the biosorbent was observed by scanning electron microscopy (SEM) on a Zeiss EVO

Table 1
Physicochemical characteristics of the biosorbent

Particle size (μm)	315–400
d_p (μm)	357.5
ρ_{app} (g/cm^3)	0.43
S_p (m^2/g)	0.039

40 EP microscope at various magnifications. Fourier transform infrared (FTIR) spectrum of the biosorbent was recorded using a Shimadzu FTIR-4800S spectrometer over the wavenumber range of 500–4,000 cm^{-1}. The samples were prepared using the conventional KBr pellet technique (1 mg of biosorbent in 300 mg of KBr).

The quantitative elemental analysis of the mineral fraction of the biosorbent was performed using a Shimadzu RF-1501 XRF spectrometer. The mineral fraction was obtained by heating the dried residue at about 400˚C in air for 3 h for the total degradation of organic matter.

2.1.2.3. Acid-base potentiometric titration. Ion exchange properties of the biosorbent regarding H^+ and OH^- ions were studied by potentiometric titration at ambient temperature following the procedure described by Chubar et al. [34]. The aliquots of fungal residue (1 g dry wt.) were introduced into magnetically stirred Erlenmeyer flasks containing 0.05 L of 0.1 M KNO_3 solution. After stirring for 2 h, precise volumes of 0.1 M HCl or 0.1 M NaOH were added to the flasks. The stirring was maintained for 24 h and the equilibrium pH was measured (Hanna 211 pH-meter). The relative ion exchange capacity (IEC) of the biosorbent (meq/g) was calculated according to:

$$\mathrm{IEC} = \frac{C(V - v)}{m} \tag{2}$$

where C (mol/L) is the concentration of HCl or NaOH solution added, V (L) is the volume of HCl or NaOH solutions added to the biosorbent suspension, v (L) is the volume of NaOH or HCl solution needed to reach the same pH in blank experiments (without biosorbent), and m (g) is the weight of biosorbent aliquots.

The overall electrical charge per gram of biosorbent was calculated as follows, considering electrical neutrality of the liquid-biomass suspension:

(1) Acid pH (HCl added):

$$Q_x^+ = \frac{F(V_o + V_a)}{m}\left(\frac{C_a V_a}{V_o + V_a} + [OH^-] - [H^+]\right) \tag{3}$$

where Q_x^+ (C/g) is the positive overall charge per unit mass of biosorbent, V_o (L) is the initial volume of liquid medium in the test flask, C_a (mol/L) and V_a (L) is the concentration and added volume of acid, respectively, $[H^+]$ and $[OH^-]$ (mol/L) are the concentrations of protons and hydroxyl ions in solution, respectively, and F is the Faraday constant ($F = 96{,}485$ C/mol).

(2) Basic pH (NaOH added):

$$Q_x^- = \frac{F(V_o + V_b)}{m}\left(\frac{C_b V_b}{V_o + V_b} + [H^+] - [OH^-]\right) \tag{4}$$

where Q_x^- (C/g) is the negative overall charge per unit mass of biosorbent, and C_b (mol/L) and V_b (L) are the concentration and added volume of base, respectively.

2.2. Column study

Fig. 1 shows a schematic diagram of the setup for the continuous adsorption study. The fixed-bed column was made of a glass tube with a length of 25 and 1.5 cm internal diameter. The biosorbent particles were packed inside the column until the desired depth was reached. The biosorbent bed was supported and closed by glass wool and glass beads to improve the flow distribution. The effluent feed solution was fed through the column by a peristaltic pump in an up-flow mode to avoid the channeling of solution and compaction. Samples were collected from the exit of the column at different time intervals and analyzed for the remaining cadmium concentrations by atomic absorption spectroscopy. The flow to the column was continued until the outlet concentration (C_t) approached the inlet concentration (C_0). The experiments were carried out at room temperature (20 ± 2˚C) by varying operating conditions such as the flow rate, inlet concentration, and bed depth. All experiments were performed in duplicates and the deviations were within 5%. For all breakthrough curves, the mean values were used.

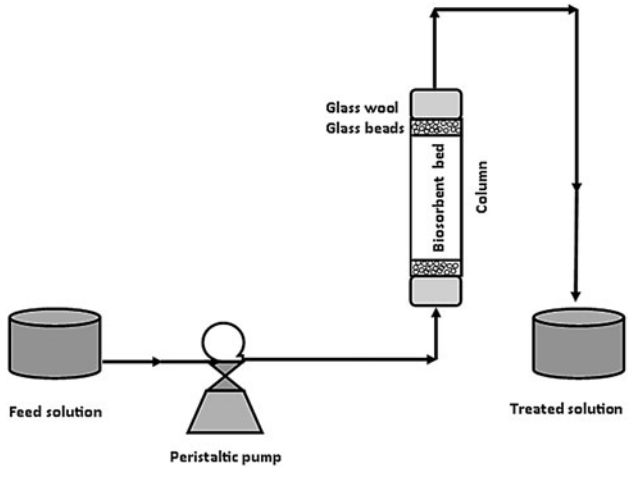

Fig. 1. Experimental system for column biosorption.

The cadmium uptake in the bed q is calculated from the area under the breakthrough curve using the following equation:

$$q = \frac{Q}{1,000\ m}\left(C_0 t_s - \int_0^{t_s} C\ dt\right) \quad (5)$$

where C and C_0 (mg/L) are the initial and effluent concentrations at time t, respectively. q (mg/g) is the biosorption capacity of the bed, t_s (min) is the exhaustion time, Q (mL/min) is the flow rate, and m (g) is the mass of biosorbent.

2.3. Regeneration and reusability tests

After the column reached exhaustion ($Q = 10$ mL/min, $Z = 15$ cm, and $C_0 = 50$ mg/L), the biosorbent was regenerated using 0.05 M HNO_3 with the flow rate adjusted to 10 mL/min. Deionized water was used to wash the bed until the pH of the effluent solution was stabilized near 7.0. The column was again fed with a synthetic solution containing 50 mg/L of Cd(II). The four cycles of biosorption followed by desorption were performed to evaluate the reuse potential of the biosorbent.

2.4. Modeling of breakthrough curves

The mathematical models such as Thomas, Adams–Bohart, and BDST are the most used to describe the dynamic behavior of pollutants' removal in a fixed-bed column. Therefore, these models were applied to the experimental data obtained for biosorption of cadmium by *P. mutilus* at various operating conditions.

2.4.1. The Thomas model

The Thomas model is the most widely used model in column performance theory. The model assumes second-order reversible reaction kinetics and the Langmuir isotherm [35,36]. This approach focused on the estimation of characteristic parameters such as maximum removal capacity (q_0) and the reaction rate constant (k_{Th}). The linearized form of Thomas model can be expressed as Eq. (6).

$$\ln\left(\frac{C_0}{C_t} - 1\right) = \frac{k_{Th}}{Q}(q_0 x - C_0 V_{eff}) \quad (6)$$

where k_{Th} (L/mg min) is the Thomas rate constant, C_0 and C_t (mg/L) are the inlet and outlet concentrations, Q (mL/min) is the flow rate, q_0 (mg/g) is the maximum biosorption capacity, x (g) is the amount of biosorbent in the bed, V_{eff} (mL) is the effluent volume, and $V_{eff} = Q/t$, t (min) is the operating time.

A linear plot of ln $[(C_0/C_t) - 1]$ against time (t) was employed to determine the values of k_{Th} and q_0 from the intercept and slope of the plot [37].

2.4.2. The Adams–Bohart model

The Adams–Bohart model is usually used for the description of the initial part of the breakthrough curve [38,39]. It is based on the surface reaction rate theory and assumes that the adsorption rate is proportional to both the concentration of the adsorbate and the residual adsorptive capacity of the adsorbent [35].

The expression for the linear Adams–Bohart model is as follows [40,41]:

$$\ln\left(\frac{C_t}{C_0}\right) = k_{AB} C_0 t - k_{AB} N_0 \left(\frac{Z}{F}\right) \quad (7)$$

where k_{AB} (L/mg min) is the biosorption rate constant, N_0 (mg/L) is the saturation concentration, F (cm/min) is the linear velocity calculated by dividing the flow rate by the column section area, and Z (cm) is the bed depth. The parameters k_{AB} and N_0 can be calculated from the intercept and slope of the linear plot of ln (C_t/C_0) against t (not shown in figure).

2.4.3. BDST model

The BDST model is one of the most simplified fixed-bed analysis methods, which is implemented in many adsorption column studies [42,43]. It was proposed by Bohart and Adams, and subsequently modified by Hutchins [44]. The model is based on physically measuring the capacity of the bed at different breakthrough values, while ignoring the intraparticle mass transfer resistance and the external film resistance such that the adsorbate is directly adsorbed on the adsorbent surface [45].

Hutchins proposed a linear relationship between the bed depth and service time, called BDST model (Eq. (8)) [46].

$$t_b = \frac{N_b}{C_0 F} Z - \frac{1}{K_a C_0} \ln\left(\frac{C_0}{C_b} - 1\right) \quad (8)$$

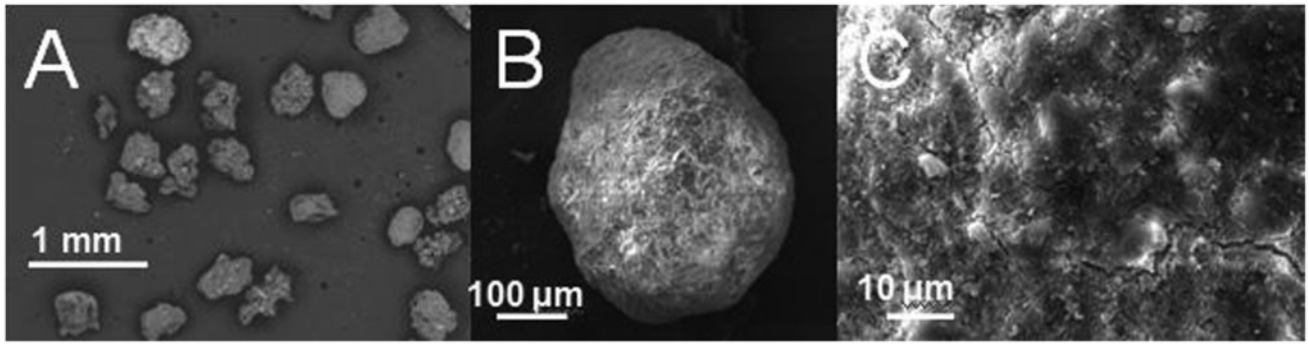

Fig. 2. Scanning electron micrographs of the biosorbent particles. Different magnifications were applied; (A) 1 mm, (B) 100 µm, and (C) 10 µm.

where t_b (min) is the service time at a breakthrough point, C_0 (mg/L) is the initial concentration, C_b (mg/L) is the breakthrough concentration, K_a (L/mg min) is the rate constant, N_b (mg/L) is the saturation concentration, F (cm/min) is the linear velocity, and Z (cm) is the bed depth.

A plot of time (t_b) against bed depth (Z) was employed to determine the parameters N_0 and K_a from the intercepts and slopes.

3. Results and discussion

3.1. Biosorbent characterization

3.1.1. SEM, FTIR, and X-ray fluorescence (XRF) analyses

From Fig. 2, the SEM images of the dried biosorbent indicate a regular spherical morphology with an external surface that, although rather smooth, displayed a number of cracks likely to favor solute biosorption through enhanced diffusion to active sites.

From Table 2, the main elements present in the mineral fraction are calcium, silicon, phosphorus, and, to a lesser extent, iron and potassium at various amounts of 42.9, 36.9, 13.4, 4.1, and 2.3% (w/w) of the dry weight, respectively (Table 2).

Table 2
XRF analysis of the mineral fraction of the biosorbent

Element	% (w/w)[a]
Ca	42.9
Si	36.9
P	13.4
Fe	4.1
K	2.3
Zn	0.2
Others	0.2

[a]Mean of two analyses.

In order to identify the main functional groups of the biosorbent, including those involved in the biosorption process, FTIR analysis of the biosorbent was also performed. Fig. 3 shows the FTIR spectrum of the biosorbent, the vibration frequencies, and their corresponding groups. The obtained results indicate the presence of hydroxyl groups (–OH) (glycoproteins), amino groups (–NH) (amino acids and glycoproteins), and carboxyl groups (C=O, C–O) (carboxylic acids, fatty acids, and primary and secondary amides) (Fig. 3).

3.1.2. Acid-base potentiometric titration

The pH-dependence of both the IEC of the biosorbent and its overall electrical charge obtained from Eqs. (2)–(4) are shown in Fig. 4. At low pH values, the IEC decreased as the pH increased to reach a minimum at a pH of 8, and then increased again at higher pH. This indicates the amphoteric nature of the biosorbent, which can be explained by the existence of weak acid and basic groups on the biosorbent. At low pH, the residue behaved like a base and an anion

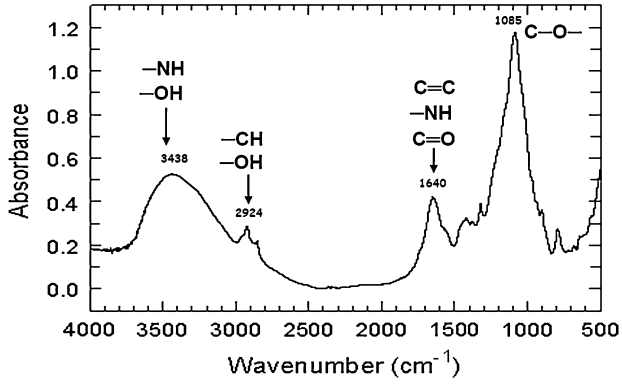

Fig. 3. Infrared spectrum of the biosorbent.

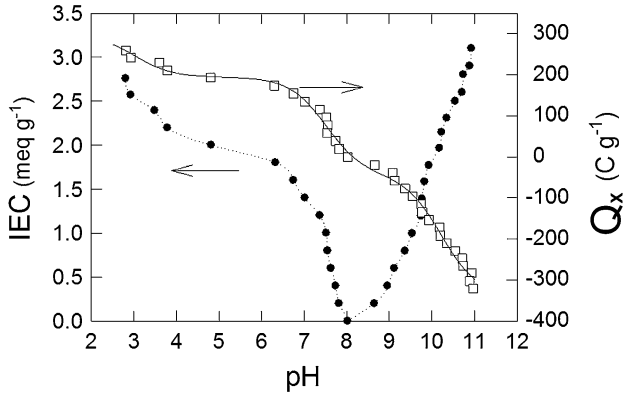

Fig. 4. The pH-dependence of IEC and overall electrical charge (Q_x) of the biosorbent.

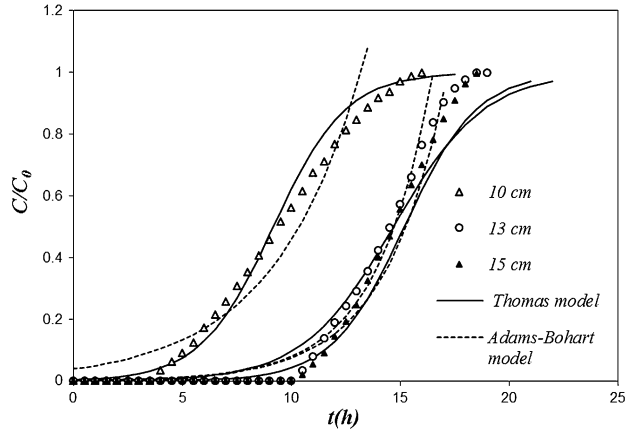

Fig. 5. Comparison of the experimental and predicted breakthrough curves obtained at various bed depths according to the Adams–Bohart and Thomas models (initial concentration: 50 mg/L and flow rate: 20 mL/min).

exchanger, primarily owing to the protonation of amino groups provided by proteins, and acid groups being neutral or partially negative. Therefore, the biosorbent remained positively charged.

At a pH value of 8, the overall electric charge and IEC of the biosorbent were close to zero (Fig. 4) due to the charge balance that occurs between the positively charged amino groups and the deprotonated negatively charged acid groups. At higher pH, the residue behaves as an acid, yielding hydrogen ions from the still undissociated groups. Its cation exchange capacity and negative charge increased with pH.

3.2. Effect of operating parameters on column performance

The continuous flow biosorption of cadmium onto *P. mutilus* biomass was investigated as a function of flow rate, bed depth, and inlet concentration of cadmium. During the experiments, the studied parameter was varied while other parameters were kept constant. They were performed at room temperature (20°C ± 2) at a pH of 4. The shape of breakthrough curves for various operating conditions was compared using a plot of dimensionless concentration (C/C_0) vs. time (t).

3.2.1. Effect of bed depth

The effect of bed depth (10, 13, and 15 cm) on the continuous biosorption of cadmium was investigated at constant flow rate and inlet concentration of 20 mL/min and 50 mg/L, respectively (Fig. 5). The detailed experimental parameters are shown in Table 3. The results showed that the biosorption capacities increased with an increase in the bed depth. It was observed also that the breakthrough and exhaustion times increased as the bed depth increased, and the biosorption process reached saturation more slowly with an increase in the bed depth from 10 to 13 and 15 cm (Fig. 5). A high-bed depth resulted in a high volume of metal solution treated and high removal of cadmium. However, there is no significant difference in the shape of breakthrough curves when the bed depth increased from 13 to 15 cm.

This behavior may be due to a longer contact time caused by more biosorbent in the column, which provided more binding sites and a larger surface for the removal of Cd(II). A similar tendency was also reported by Vimala et al. [47] for cadmium biosorption in a fixed-bed column packed with macrofungus *Pleurotus platypus*. They concluded that the breakthrough time, exhaustion time, and bed capacity increased as the bed depth increased.

3.2.2. Effect of initial concentration

The effect of varying the initial Cd(II) concentration from 20 to 50 mg/L on the shape of the breakthrough

Table 3
Experimental parameters for the biosorption of Cd(II) onto *P. mutilus* biomass

C_0 (mg/L)	Z (cm)	Q (mL/min)	t_p (h)	t_s (h)	q (mg/g)
20	15	20	15.0	23.0	78.28
40			10.0	21.0	82.34
50			5.0	16.0	84.85
20	10	20	4.5	14.5	68.69
	13		10.0	17.0	74.91
20	15	5	27.5	45.0	82.37
		10	16.5	25.0	80.12

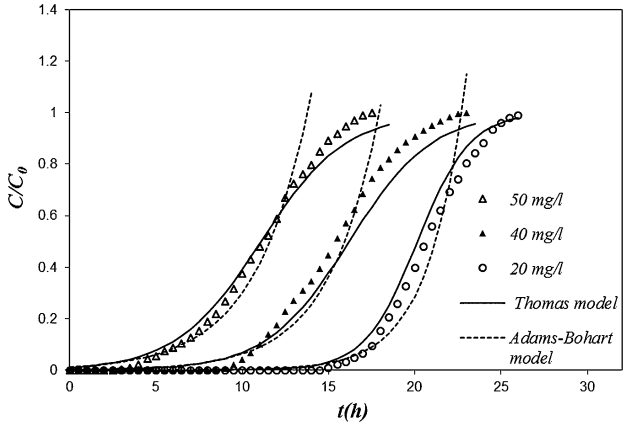

Fig. 6. Comparison of the experimental and predicted breakthrough curves obtained at various inlet concentrations according to the Adams–Bohart and Thomas models (bed depth: 10 cm and flow rate: 20 mL/min).

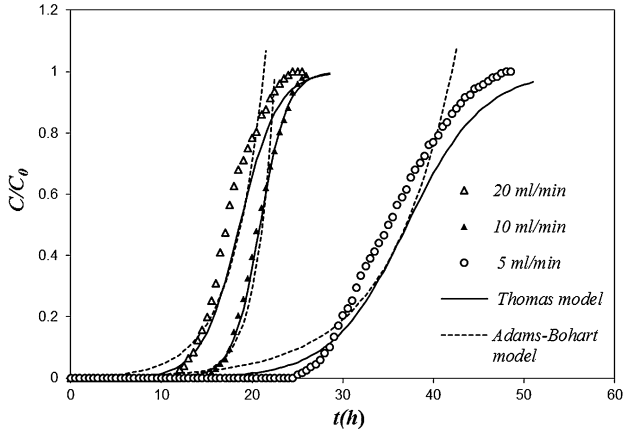

Fig. 7. Comparison of the experimental and predicted breakthrough curves obtained at various flow rates according to the Adams–Bohart and Thomas models (initial concentration: 50 mg/L and bed depth: 10 cm).

curves was investigated at a constant bed depth (15 cm) and feed flow rate (20 mL/min). The resulting breakthrough curves are shown in Fig. 6.

It appears that the breakthrough curves became shaper, breakthrough time and exhaustion points became shorter with an increase in the concentration of cadmium (Fig. 6). This result was similar to that reported in previous studies. Acheampong et al. [48] investigated the effect of influent Cu(II) concentration on breakthrough curves and found that a decrease in Cu(II) concentration obtained a later breakthrough. The tendency was also obtained by Han et al. [49]. They reported that the breakthrough time decreased and sharper breakthrough curves were obtained with an increase in the influent MB concentration.

Table 3 shows that the biosorption capacity increased slightly with an increase in the concentration of Cd(II). An increase in the inlet concentration reduced the treated volume of solution before the bed gets saturated, since high Cd(II) concentrations may saturate the biosorbent more quickly, thereby decreasing the operating time. Decreasing the Cd(II) concentration increased the volume of solution that can be treated, shifting the breakthrough curve to the right (Fig. 6). During the first 20 h of operating time, the value of C/C_0 reached 0.95, 0.76, and 0.13 when the initial concentrations were 50, 40, and 20 mg/L, respectively.

3.2.3. Effect of flow rate

The effect of flow rates from 5 to 20 mL/min on breakthrough curves can be observed in Fig. 7. The inlet concentration and bed depth were kept constant at 50 mg/L and 10 cm, respectively.

As expected, an increase in flow rate produces a reduction in breakthrough and exhaustion times, and therefore, the breakthrough curve became steeper with

Table 4
The Adams–Bohart and Thomas fitting parameters for the biosorption of Cd(II) onto *P. mutilus* biomass

Conditions			Adams–Bohart model			Thomas model		
C_0 (mg/L)	Z (cm)	Q (mL/min)	K_{BA} ($\times 10^4$) (L/mg min)	N_0 ($\times 10^{-3}$) (mg/L)	R^2	K_{Th} ($\times 10^4$) (L/mg min)	q_0 (mg/g)	R^2
20	15	20	3.85	12.51	0.930	1.41	53.20	0.983
40			1.45	26.46	0.896	1.75	73.71	0.992
50			1.06	31.18	0.956	1.54	77.50	0.978
20	10	20	2.05	17.90	0.897	2.14	51.76	0.972
	13		3.01	14.87	0.942	1.68	55.63	0.974
20	15	5	1.15	20.55	0.861	1.26	67.79	0.978
		10	2.30	14.62	0.909	1.57	55.89	0.973

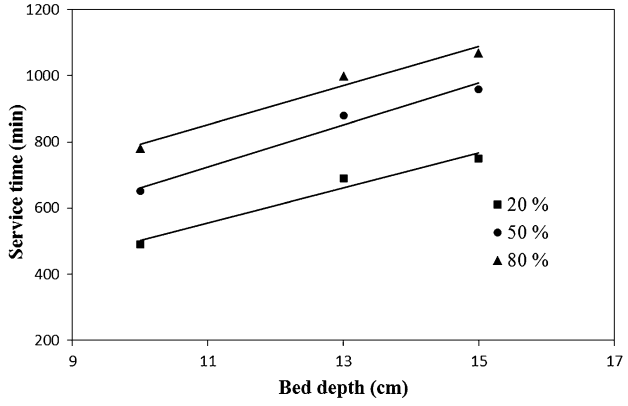

Fig. 8. BDST model for Cd(II) biosorption at various breakthrough values.

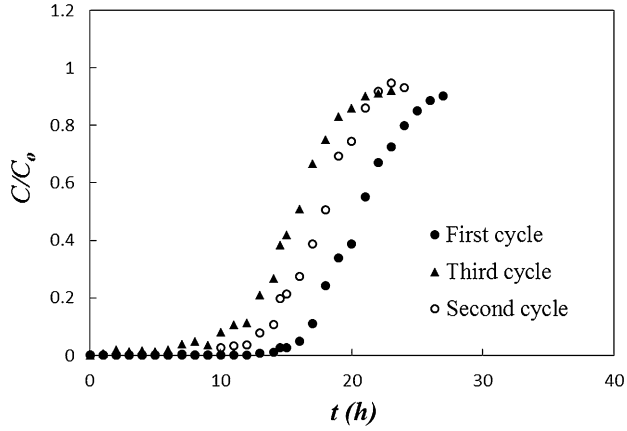

Fig. 9. Breakthrough curves obtained for three consecutive cycles of biosorption–regeneration of Cd(II) onto *P. mutilus* biomass (initial concentration: 50 mg/L, bed depth: 15 cm, and flow rate: 10 mL/min).

a shorter mass transfer zone (Fig. 7). The results in Table 3 indicate that the biosorption of cadmium onto *P. mutilus* biomass depends on flow rate. The biosorption capacity increased from 78.28 to 82.37 mg/g with a decrease in the flow rate from 20 to 5 mL/min, respectively (Table 3). At high flow rates, early breakthrough and exhaustion time resulted in a low uptake. This behavior can be explained by insufficient residence time for Cd(II) ions in the column, this did not allow the progression of their mass transfer and removal from the solution [50,51]. The result was similar to that reported by Acheampong et al. [48] during the biosorption of Cu(II) onto coconut shells in fixed-bed column. They concluded that the breakthrough curve occurs faster at higher flow rates, and the breakthrough and exhaustion times decreased with an increase in the flow rate.

3.3. Prediction of breakthrough curves

3.3.1. Thomas model

The experimental data of breakthrough curves shown in Figs. 5–7 were fitted linearly according to the Thomas model (Eq. (6)). The predicted breakthrough curves at various operating conditions are shown in Figs. 5–7. The Thomas parameters such as k_{Th} and q_0 obtained using linear regression analysis are listed in Table 4.

The results show a good agreement between the experimental and predicted breakthrough curves ($R^2 > 0.96$). From Table 4, it appears that the predicted q_0 was close to the experimental capacities of the column. As the flow rate increased, the values of k_{Th} increased while q_0 decreased, due to faster mass transfer for cadmium biosorption and a decrease in mass transfer resistance and axial dispersion [52]. Contrariwise, the values of k_{Th} decreased while those of q_0 increased with an increase in the initial concentration and bed depth. This is attributed to the driving force for biosorption in the concentration difference, and the increase in q_0 with an increase in the bed depth is due to the increase in contact time for cadmium removal.

3.3.2. The Adams–Bohart model

The experimental breakthrough curves obtained for the biosorption of Cd(II) by *P. mutilus* biomass at various operating conditions were analyzed according to the Adams–Bohart model (Eq. (7)). The plots are shown in Figs. 5–7. The kinetic parameters such as N_0,

Table 5
The BDST model parameters for the biosorption of Cd(II) onto *P. mutilus* biomass

C/C_0	a (min/cm)	b (min)	K_a (L/mg min)	N_b (mg/L)	R^2
0.2	53.16	−30.94	8.96×10^{-4}	30,115.14	0.952
0.5	57.28	32.14	0	32,449.12	0.976
0.8	63.21	200.63	2.22×10^{-5}	35,808.46	0.961

Table 6
Biosorption and regeneration parameters for three successive biosorption–regeneration cycles

Cycle	q (mg/g)	t_p (h)	t_s (h)	Removal (%)	M_{total} (mg)	M_{ad} (mg)	Regeneration efficiency (%)
1	80.63	17	27	86.36	810	699.51	91.64
2	68.67	14	23	79.04	690	545.38	92.87
3	2.67	11	21	72.91	630	459.33	91.09

and k_{AB} obtained are shown in Table 4. The results obtained in Figs. 5–7 show that the Adams–Bohart model provided a poor fitting compared to the Thomas model ($R^2 < 0.96$). The predicted k_{AB} decreased while N_0 increased with an increase in theC_0 (Table 4), which indicates that the overall system kinetic was dominated by the external mass transfer in the initial part of biosorption in the column [53,54]. As the flow rate and bed depth increased, the values of N_0 decreased and k_{BA} increased, due to the decrease in mass transfer resistance and the axial dispersion in the packed bed [52]. The decrease in N_0 with an increase in the flow rates is due to the decrease of the residence time of Cd(II) ions in the column because the biosorption capacity for the continuous flow process is directly proportional to the contact time.

3.3.3. BDST model

The results of bed depth (Z) and service time at breakthrough point (t_b) are plotted in Fig. 8 according to Eq. (8) for 20, 50, and 80% breakthrough. The slope, intercept, R^2, saturation concentration (N_0), and rate constant (K_a) are listed in Table 5. Fig. 8 shows the linear t_b vs. Z plot of the breakthrough data obtained at various bed depths, indicating the validity of the BDST model for biosorption system studied with high-correlation coefficients ($R^2 > 0.94$). Therefore, the BDST model could be applied for all breakthrough values to describe the whole breakthrough curves of Cd(II) biosorption onto *P. mutilus* biomass. From Table 5, as the values of C_t/C_0 increased, the biosorption capacity of the bed per unit bed volume N_0, the slope, and the intercept increased. The results are similar to those obtained by Han et al. [49] during the adsorption of methylene blue by phoenix tree leaf powder in a fixed-bed column. The BDST model parameters can be useful to further scale up the process for other flow rates without further experimental runs.

3.4. Regeneration and reusability tests

In order to test the biosorbent reusability, the *P. mutilus* biomass was reused for three biosorption–regeneration cycles. Fig. 9 shows the breakthrough curves obtained for each biosorption cycle, and their corresponding breakthrough time, exhaustion time, and column uptake are listed in Table 6. The results show a slight decrease in breakthrough and exhaustion times as the regeneration cycles progressed, resulting in a broadened mass transfer zone. Furthermore, the biosorption capacity and removal efficiency slightly decreased with regeneration cycles (Table 6). The regeneration efficiencies were greater than 90% in all the cycles, which can be explained by the gradual deterioration of the biomass on continuous usage.

4. Conclusion

The *P. mutilus* macrofungal biomass displayed promising characteristics as a potential biosorbent to remove Cd(II) from contaminated water, among which are a low cost (waste material with no pretreatment needed) together with high biosorption capacity. Based on the experimental results, the following conclusions can be listed:

(1) *P. mutilus* macrofungal biomass could be used as an effective biosorbent to remove Cd(II) in a fixed-bed column.
(2) The continuous flow biosorption of Cd(II) is dependent on the flow rate, inlet concentration, and bed depth. An increase in bed depth provides an increase in the treated volume and a slight reduction in the biosorption capacity. As the flow rate decreased, the treated volume and biosorption capacity increased. At high inlet concentrations, the biosorption capacity also increased.
(3) The Thomas model described the breakthrough curves far better than the Adams–Bohart model. The BDST model was successfully applied to the experimental data at various breakthrough values, suggesting prospective use of *P. mutilus* macrofungal biomass for the high removal of Cd(II) in continuous mode.
(4) The biosorbent was easily regenerated using 0.05 M HNO_3 solution and efficiently reused for three successive biosorption–regeneration cycles.

Nomenclature

C_a — concentration of acid (mg/L)
C_b — concentration of base (mg/L)
C_0 — inlet feed concentration (mg/L)
C_t — effluent concentration at time t (mg/L)
C_e — effluent concentration at equilibrium (mg/L)
d_p — mean diameter of biosorbent particles (μm)
F — linear velocity calculated by dividing the flow rate by the column section area (cm/min)
K_a — rate constant in the BDST model (L/mg min)
k_{AB} — biosorption rate constant of the Adams–Bohart model (L/mg min)
k_{Th} — Thomas rate constant (L/min mg)
q_e — biosorption capacity at equilibrium (mg/g)
q — biosorption capacity at time t (mg/g)
q_0 — maximum biosorption capacity of the biosorbent (mg/g)
Q — flow rate (mL/min)
Q_x — overall electrical charge per unit mass of biosorbent (C/g)
Q_x^+ — positive overall charge per unit mass of biosorbent
Q_x^- — negative overall charge per unit mass of biosorbent
M — mass of the biosorbent (g)
N_0 — saturation concentration according to the Adams–Bohart model (mg/g)
N_b — saturation concentration according to the BDST model (mg/g)
R^2 — regression coefficient
S_p — specific surface area of the biosorbent (m^2/g)
t — time (min)
t_p — breakthrough time (min)
t_s — exhaustion time (min)
V_o — initial volume of liquid medium in the test flask (L)
V_a — added volume of acid (L)
V_b — added volume of base (L)
V — volume of NaOH or HCl solution added to the biosorbent suspension (L)
V_{eff} — effluent volume (mL)
x — biosorbent amount in the column (g)
Z — bed depth of the column (cm)
v — volume of NaOH or HCl solution needed to reach the same pH in blank experiments (without biosorbent) (L)
ρ_{app} — apparent density of the biosorbent (g/mL)

References

[1] S.S. Pillai, B. Deepa, E. Abraham, N. Girija, P. Geetha, L. Jacob, M. Koshy, Biosorption of Cd(II) from aqueous solution using xanthated nano banana cellulose: Equilibrium and kinetic studies, Ecotoxicol. Environ. Saf. 98 (2013) 352–360.
[2] C. Guiqiu, Z. Guangming, T. Lin, D. Chunyan, J. Xiaoyun, H. Guohe, L. Hongliang, S. Guoli, Cadmium removal from simulated wastewater to biomass byproduct of Lentinusedodes, Bioresour. Technol. 99 (2008) 7034–7040.
[3] M.R. Bruins, S. Kapil, F.W. Oehme, Microbial resistance to metals in the environment, Ecotoxicol. Environ. Saf. 45 (2000) 198–207.
[4] E. Smit, P. Leeflang, K. Wernars, Detection of shifts in microbial community structure and diversity in soil caused by copper contamination using amplified ribosomal DNA restriction analysis, FEMS Microbiol. Ecol. 23 (1997) 249–261.
[5] H. Doshi, A. Ray, I. Kothari, Biosorption of cadmium by live and dead spirulina: IR spectroscopic, kinetics, and SEM studies, Curr. Microbiol. 54 (2007) 213–218.
[6] WHO, Guidelines for drinking water quality: Recommendations, third ed., vol. 1, World Health Organization, Geneva, 2008.
[7] C. Wong, J.P. Barford, G. Chen, G. McKay, Kinetics and equilibrium studies for the removal of cadmium ions by ion exchange resin, J. Environ. Chem. Eng. 2 (2014) 698–707.
[8] Et. Ennaassia, K. El Kacemi, A. Kossir, G. Cote, Study of the removal of Cd(II) from phosphoric acid solutions by precipitation of CdS with Na_2S, Hydrometallurgy. 64 (2002) 101–109.
[9] R. Liu, B. Liu, L. Zhu, Z. He, J. Ju, H. Lan, H. Liu, Effects of fluoride on the removal of cadmium and phosphate by aluminum coagulation, J. Environ. Sci. 32 (2015) 118–125.
[10] N. Pont, V. Salvadó, C. Fontàs, Selective transport and removal of Cd from chloride solutions by polymer inclusion membranes, J. Membr. Sci. 318 (2008) 340–345.
[11] K.N. Han, B.Y. Yu, S.Y. Kwak, Hyperbranched poly(amidoamine)/polysulfone composite membranes for Cd(II) removal from water, J. Membr. Sci. 396 (2012) 83–91.
[12] A.H. Sulaymon, A.O. Sharif, T.K. Al-Shalchi, Removal of cadmium from simulated wastewaters by electrodeposition on stainless steeel tubes bundle electrode, Desalin. Water. Treat. 29 (2011) 218–226.
[13] M. Kobya, E. Demirbas, E. Senturk, M. Ince, Adsorption of heavy metal ions from aqueous solutions by activated carbon prepared from apricot stone, Bioresour. Technol. 96 (2005) 1518–1521.
[14] B. Volesky, Biosorption and me: A review, Water. Res. 41 (2007) 4017–4029.
[15] I. Kula, M. Uğurlu, H. Karaoğlu, A. Çelik, Adsorption of Cd(II) ions from aqueous solutions using activated carbon prepared from olive stone by $ZnCl_2$ activation, Bioresour. Technol. 99 (2008) 492–501.
[16] M.H. Givianrad, M. Rabani, M. Saber-Tehrani, P. Aberoomand-Azar, M. Hosseini Sabzevari, Preparation and characterization of nanocomposite, silica aerogel, activated carbon and its adsorption properties for Cd(II) ions from aqueous solution, J. Saudi Chem. Soc. 17 (2013) 329–335.
[17] G.G. Stavropoulos, A.A. Zabaniotou, Minimizing activated carbons production cost, Fuel. Process. Technol. 90 (2009) 952–957.
[18] D. Guo, Q. Shi, B. He, X. Yuan, Different solvents for the regeneration of the exhausted activated carbon used in the treatment of coking wastewater, J. Hazard. Mater. 186 (2011) 1788–1793.
[19] H. Tounsadi, A. Khalidi, M. Abdennouri, N. Barka, Biosorption potential of *Diplotaxis harra* and *Glebionis*

coronaria L. biomasses for the removal of Cd(II) and Co(II) from aqueous solutions, J. Environ Chem. Eng. 3 (2015) 822–830.
[20] N. Barka, M. Abdennouri, M. El Makhfouk, S. Qourzal, Biosorption characteristics of cadmium and lead onto eco-friendly dried cactus (*Opuntia ficusindica*) Cladodes, J. Environ. Chem. Eng. 1 (2013) 144–149.
[21] N. Barka, M. Abdennouri, A. Boussaoud, M. El Makhfouk, Biosorption characteristics of cadmium(II) onto *Scolymus hispanicus* L. as low-cost natural biosorbent, Desalination 258 (2010) 66–71.
[22] P. Arivalagan, D. Singaraj, V. Haridass, T. Kaliannan, Removal of cadmium from aqueous solution by batch studies using *Bacillus cereus*, Ecol. Eng. 71 (2014) 728–735.
[23] A. Chatterjee, S. Schiewer, Multi-resistance kinetic models for biosorption of Cd by raw and immobilized citrus peels in batch and packed-bed columns, Chem. Eng. J. 244 (2014) 105–116.
[24] A.M. Awwad, N.M. Salem, Kinetics and thermodynamics of Cd(II) biosorption onto loquat (*Eriobotrya japonica*) leaves, J. Saudi Chem. Soc. 18 (2014) 486–493.
[25] R.A.K. Rao, M.A. Khan, F. Rehman, Utilization of Fennel biomass (*Foeniculum vulgari*) a medicinal herb for the biosorption of Cd(II) from aqueous phase, Chem. Eng. J. 156 (2010) 106–113.
[26] G. Mahajan, D. Sud, Application of ligno-cellulosic waste material for heavy metal ions removal from aqueous solution, J. Environ. Chem. Eng. 1 (2013) 1020–1027.
[27] A. Chergui, R. Kerbachi, G.A. Junter, Biosorption of hexacyanoferrate(III) complex anion to dead biomass of the basidiomycete *Pleurotus mutilus*: Biosorbent characterization and batch experiments, Chem. Eng. J. 147 (2009) 150–160.
[28] N. Yeddou-Mezenner, Kinetics and mechanism of dye biosorption onto an untreated antibiotic waste, Desalination 262 (2010) 251–259.
[29] S. Moussous, A. Selatnia, A. Merati, G.A. junter, Batch cadmium(II) biosorption by an industrial residue of macrofungal biomass (*Clitopilus scyphoides*), Chem. Eng. J. 197 (2012) 261–271.
[30] S. Singh, V.C. Srivastava, I.D. Mall, Fixed-bed study for adsorptive removal of furfural by activated carbon, Colloids. Surf., A 332 (2009) 50–56.
[31] F.W. Sousa, A.G. Oliveira, J.P. Ribeiro, M.F. Rosa, D. Keukeleire, R.F. Nascimento, Green coconut shells applied as adsorbent for removal of toxic metal ions using fixed-bed column technology, J. Environ. Manage. 91 (2010) 1634–1640.
[32] A.A. Ahmad, B.H. Hameed, Fixed-bed adsorption of reactive azo dye onto granular activated carbon prepared from waste, J. Hazard. Mater. 175 (2010) 298–303.
[33] K. Chandra Sekhar, C.T. Kamala, N.S. Chary, Y. Anjaneyulu, Removal of heavy metals using a plant biomass with reference to environmental control, Int. J. Miner. Process. 68 (2003) 37–45.
[34] N. Chubar, J.R. Carvalho, M.J. Neiva Correia, Cork biomass as biosorbent for Cu(II), Zn(II) and Ni(II), Colloid. Surf., A 230 (2003) 57–65.
[35] M. Trgo, N.V. Medvidovic, J. Peric, Application of mathematical empirical models to dynamic removal of lead on natural zeolite clinoptilolite in a fixed bed column, Indian J. Chem. Technol. 18 (2011) 123–131.
[36] Z. Xu, J.G. Cai, B.-C. Pan, Review: Mathematically modeling fixed-bed adsorption in aqueous systems, J. Zhejiang. Univ. Sci. A. 14 (2013) 155–176.
[37] G. Yan, T. Viraraghavan, Heavy metal removal in a biosorption column by immobilized *M. rouxii* biomass, Bioresour. Technol. 78 (2001) 243–249.
[38] A.P. Lim, A.Z. Aris, Continuous fixed-bed column study and adsorption modeling: Removal of cadmium (II) and lead (II) ions in aqueous solution by dead calcareous skeletons, Biochem. Eng. J. 87 (2014) 50–61.
[39] B. Salamatinia, A.H. Kamaruddin, A.Z. Abdullah, Modeling of the continuous copper and zinc removal by sorption onto sodium hydroxide-modified oil palm frond in a fixed-bed column, Chem. Eng. J. 145 (2008) 259–266.
[40] P.B. Bhakat, A.K. Gupta, S. Ayoob, Feasibility analysis of As(III) removal in a continuous flow fixed bed system by modified calcined bauxite (MCB), J. Hazard. Mater. 139 (2007) 286–292.
[41] J.L. Gong, Y.L. Zhang, Y. Jiang, G.M. Zeng, Z.H. Cui, K. Liu, C. Hui Deng, Q.Y. Niu, J.H. Deng, S.Y. Huan, Continuous adsorption of Pb(II) and methylene blue by engineeredgraphite oxide coated sand in fixed-bed column, Appl. Surf. Sci. 330 (2015) 148–157.
[42] V.K.C. Lee, J.F. Porter, G. McKay, Modified design model for the adsorption of dye onto peat, Inst. Chem. Eng. Part C, Food Bioprod. Process. 79 (2001) 21–26.
[43] K. Santhy, P. Selvapathy, Removal of reactive dyes from wastewater by adsorption on coir pith activated carbon, Bioresour. Technol. 97 (2006) 1329–1336.
[44] R.A. Hutchins, New method simplifies design of activated carbon systems, Chem. Eng. 80 (1973) 133–138.
[45] D.C.K. Ko, J.F. Porter, G. McKay, Optimised correlations for the fixed bed adsorption of metal ions on bone char, Chem. Eng. Sci. 55 (2000) 5819–5829.
[46] S. Baral, N. Das, T.S. Ramulu, S.K. Sahoo, Removal of Cr(VI) by thermally actived weed *Salvinia cucullatta* on a fixed bed column, J. Hazard. Mater. 161 (2009) 1427–1435.
[47] R. Vimala, D. Charumathi, N. Das, Packed bed column studies on Cd(II) removal from industrial wastewater by macrofungus *Pleurotus platypus*, Desalination 275 (2011) 291–296.
[48] M.A. Acheampong, K. Pakshirajan, A.P. Annachhatre, P.N.L. Lens, Removal of Cu(II) by biosorption onto coconut shell in fixed-bed column systems, J. Ind. Eng. Chem. 19 (2013) 841–848.
[49] R.P. Han, Y. Wang, X. Zhao, Y.F. Wang, F.L. Xie, J.M. Cheng, M.S. Tang, Adsorption of methylene blue by phoenix tree leaf powder in a fixed-bed column: Experiments and prediction of breakthrough curves, Desalination 245 (2009) 284–297.
[50] W.H. Zou, L. Zhao, L. Zhu, Adsorption of uranium (VI) by grapefruit peel ina fixed-bed column: experiments and prediction of breakthrough curves, J. Radioanal. Nucl. Chem. 295 (2013) 717–727.
[51] Md. Tamez Uddin, Md. Rukanuzzaman, Md. Maksudur Rahman Khan, Md. Akhtarul Islam,

Adsorption of methylene blue from aqueous solution by jack-fruit (Artocarpus heteropyllus) leaf powder: A fixed-bed column study, J. Environ. Manage. 90 (2009) 3443–3450.

[52] V. Sivasankar, T. Ramachandramoorthy, A. Chandramohan, Fluoride removal from water using activated and MnO_2-coated Tamarind Fruit (*Tamarindus indica*) shell: Batch and column studies, J. Hazard. Mater. 177 (2010) 719–729.

[53] S.H. Chen, Q.Y. Yue, B.Y. Gao, Q. Li, X. Xu, K.F. Fu, Adsorption of hexavalent chromium from aqueous solution by modified corn stalk: A fixed-bed column-study, Bioresour. Technol. 113 (2012) 114–120.

[54] R. Sharma, B. Singh, Removal of Ni(II) ions from aqueous solutions using modified rice straw in a fixed bed column, Bioresour. Technol. 146 (2013) 519–524.